ORIGINAL PAPER

A calcium ion-imprinted porous film prepared from a cellulose-alginate composite

Yong Wang · Shiqin Zhu · Yunying Liao · Xiaopeng Xiong

Abstract An ion-imprinted (IIP) film has been successfully prepared in this work. Firstly, mixture solution of cellulose and alginate was obtained by dissolving those polymers in a NaOH/urea aqueous solution. Then the mixture solution was cast onto glass plate and coagulated in $CaCl_2$ aqueous solution bath to prepare a composite film. The matrix of the film was further fixed by cross-linking. Finally, the chelated Ca^{2+} in the matrix was removed to obtain the IIP film. The IIP film was characterized to show satisfactory mechanical properties, and to exhibit porous mesh network microstructure. The equilibrium swelling ratio of the IIP film was determined to be 700 %. The IIP film was immersed into Ca^{2+}, Ca^{2+}/Cu^{2+}, Ca^{2+}/Zn^{2+} and Ca^{2+}/Mg^{2+} solutions to check the adsorption behavior, respectively. The results indicate that the IIP film displayed highly selective Ca^{2+} recognition, and the presence of additional cations had little effect on the Ca^{2+} recognition. Thus prepared Ca^{2+} imprinted film have potential applications in fields such as hard water softening, and Ca^{2+} enrichment or recognition.

Keywords Regenerate cellulose · Sodium alginate · Porous film · Ion-imprinting · Selective recognition

Introduction

Molecular imprinting technique is a process through templating a special target molecule for selective recognizing specific chemical species [1]. Due to the specific recognition and the feasibility, molecularly imprinted polymers (MIP) based on this technique have attracted extensive attention and been widely applied in many fields such as chromatography, sensor device, membrane separation, and enzyme catalysis [2–5]. For example, Xu et al. [3] have prepared a porous MIP for solid-phase extraction of triazines in soil. If the MIP is porous film material, it will combine the advantages of MIP as well as the membrane separation. In other words, the material will have a huge space of target molecule exchange for MIP together with high separation efficiency of membrane [2].

Lately [6–14], a characteristic ion rather than a targeted molecule has been used as template for the preparation of porous MIP. The obtained ion imprinting polymer (IIP) is thus to have the specific ion recognition, which has been used for toxic ion removal [6–8] or for analyte enrichment [9–14]. The ion-recognition of the IIP is similar as that of MIP, namely the special groups in the matrix of the IIP would have specific interaction like chelating interaction with the designated ion. However, the preparation of IIP often requires complex synthesis condition. For example, Zhen et al. [9] employed graft polymerization combining with chemical modification to have prepared an ion-imprinted microporous polypropylene film for the selective removal of Cu^{2+}. A Ni^{2+} IIP of porous polyvinylidene fluoride film was synthesized via copolymerization, with the in situ templating ion of Ni^{2+} and dithizone as chelating ligand cross-linked in the film matrix [10]. The separation factor of the IIP film for the Ni^{2+} ion versus Co^{2+} ion was 2.6 [10]. However, it has been claimed that some disadvantages were employed during the polymerization process of the IIP preparation [8, 15], i.e. the densely cross-linked matrix would limit the activity of the deeply embedded binding sites of the IIP. On the contrary, porous structure and swollen-able network of the IIP would facilitate the affinity and capacity of the imprinted polymer toward the template target.

Sodium alginate (SA), a natural polymer widely derived from brown algae and consisting of 1,4-linked D-manuronic and L-guluronic acid residues, has been extensively

Y. Wang · S. Zhu · Y. Liao · X. Xiong (✉)
Department of Materials Science and Engineering, College of
Materials, Xiamen University, Xiamen 361005, China
e-mail: xpxiong@xmu.edu.cn

investigated and applied in biomedical fields due to its bio-compatibility, low toxicity and relatively low cost [16]. An important feature of alginate is its gelation behavior in the presence of divalent cations such as Ca^{2+}. The divalent cations are believed to bind solely to guluronate blocks along alginate chains to form "egg-box" [17, 18], suggesting the Ca^{2+} recognition ability of SA. If the Ca^{2+} was removed by stronger chelators such as ethylenediaminetetraacetic acid disodium salt dihydrate (EDTA) [19], Ca^{2+} recognition caves would be left in the SA matrix.

It has been reported [20–22] that cellulose and SA were miscible at the molecular scale, and the obtained blend films displayed porous mesh network structure to have satisfactory heavy metal ion adsorption and high equilibrium swelling ratio. Therefore, the blend system could provide an ideal matrix for IIP preparation, where the porous mesh network structure would facilitate the diffusion and recognition of solutes [8, 15] and the stiff cellulose chains [23, 24] would strengthen the obtained material. Therefore, cellulose and alginate were solution blended in a co-solvent of NaOH/urea aqueous solution and cast onto glass plate, and then were coagulated in $CaCl_2$ aqueous solution bath to prepare a blend film. The film was further fixed by cross-linking. After that, the chelated Ca^{2+} was removed to obtain the IIP film. The microstructure and the properties of the IIP film were characterized, and its selective Ca^{2+} recognition was measured in presence of competitive cations. The results indicate that the prepared Ca^{2+} IIP films have potential applications in fields such as hard water softening, and Ca^{2+} enrichment or recognition.

Experimental

Materials

Cotton linter (cellulose) with viscosity-average molecular mass (M_η) of 1.01×10^5 g/mol [25] was supplied by Hubei Chemical Fiber Group Ltd (Xiangfan, China). Sodium alginate (SA) with weight-average molecular weight (M_w) of 7×10^4 g/mol was purchased from Xiamen Renchi Chemical Industry Co. Ltd (Xiamen, China). Analytical-grade epichlorohydrin (ECH), ethylenediaminetetraacetic acid disodium salt dihydrate (EDTA), calcium chloride ($CaCl_2$), magnesium chloride ($MgCl_2$), copper chloride ($CuCl_2$), zinc chloride ($ZnCl_2$) were purchased from Sinopharm Chemical Reagent Co., Ltd (Shanghai, China), and were used as received.

Film preparation

Cellulose solution was prepared according to previous work [23]. Briefly, mixture solvent containing 7 wt.% NaOH, 12 wt.% urea and 91 wt.% water was pre-cold to −12 °C,

and then cotton linter was dispersed into the mixture solvent with vigorously stirring for 5 min. The resultant slurry was centrifuged at 6000 rpm for 8 min to obtain the upper layer transparent solution with a cellulose concentration of 3 wt.%. SA was dissolved in the same solvent with stirring for 10 h at room temperature to have a 6 wt.% polymer concentration. The cellulose and the SA solutions were mixed under ice-bath to produce a homogeneous solution with the weight ratio of 3:1 for cellulose to SA.

The polymer mixture solution was cast onto glass plate, and then exposed in air at ambient condition for 30 min. After that, the plate was immersed into a 3 wt.% $CaCl_2$ aqueous solution coagulant bath for 10 min. The peeled-off film was washed with de-ionized water for 3 times, and then immersed into 3 wt.% epichlorohydrin solution at 60 °C for 2 h, where the pH was adjusted to 12 with NaOH. [22] The film was then washed for 3 times in turn with 0.5 wt.% H_2SO_4 solution, ethanol and deionized water. After that, the film was immersed in 0.02 mol/L EDTA aqueous solution for 6 h to remove Ca^{2+}. Thus treated film was washed thoroughly with water, and finally air-dried to obtain the ion-imprinted film (IIP). The non-ion imprinted film (NIIP) was prepared through a similar procedure by directly coagulating the cellulose/SA mixture solution in 0.5 wt.% H_2SO_4 aqueous solution and then being cross-linked in 3 wt.% epichlorohydrin solution at 60 °C for 2 h. Pure regenerated cellulose film (RC) was prepared by coagulating the cellulose solution in 0.5 wt.% H_2SO_4 aqueous solution. Pure SA film was prepared by coagulating the SA aqueous solution in ethanol.

Measurements

The films before dried were frozen in liquid nitrogen, and snapped immediately, then freeze-dried. The surface and cross-section of the fractured films were coated with a thin layer of gold (about 2 nm) to observe their microstructures by using an LEO 1530 (LEO, Germany) or an XL30 (ESEM-TMP, Holland) scanning electron microscope (SEM) with 20 kV accelerating voltage.

About 0.5 g of the dried IIP and NIIP films were immersed in deionized water for desired time, and then were weighed after carefully decanting the surface water with filter paper, respectively. The swelling ratio, Q, was calculated using Eq. (1):

$$Q = (W_t - W_0)\big/ W_0 \qquad (1)$$

Where W_0 is the weight of dried film, and W_t is the weight of the wet film at time t.

The tensile strength (σ_b) and breaking elongation (ε_b) of the films in dry state were measured on an universal testing machine (WDS-5, Tianshui, Tianshui Hongshan Test

Machine Co. Ltd., Gansu, China) according to ISO 527–2, 1993 (E) at a speed of 5 mm/min.

The salts of $CaCl_2$, $MgCl_2$, $CuCl_2$, and $ZnCl_2$ were dissolved in deionized water to obtain Ca^{2+}, Ca^{2+}/Cu^{2+}, Ca^{2+}/Mg^{2+}, Ca^{2+}/Zn^{2+} mixture solutions, and their concentrations are listed in Table 1 or Table 2. About 0.1 g of the IIP and NIIP films were soaked in 10 mL Ca^{2+}, Ca^{2+}/Cu^{2+}, Ca^{2+}/Mg^{2+}, Ca^{2+}/Zn^{2+} mixture solutions with lightly stirring, respectively. After desired time, 5 mL of the supernatants were extracted. The ion concentrations (C_s) were respectively checked using an UV-visible spectrophotometer (50BIO, VARIAN, Australia) according to literature methods: Cu^{2+} with chromogenic agent of EDTA at 265 nm [26], Ca^{2+} with acid chrome blue K at 565 nm [27], Mg^{2+} with acid chrome blue K at 508 nm [27], and Zn^{2+} with Zincon at 580 nm [28].

X-ray diffraction (XRD) patterns of the films were recorded using a PANalytical diffractometer (PANalytical, Netherlands) with Cu-Kα radiation. The vacuum dried films were continuously scanned from 10° to 50° (2θ) at a speed of 0.0167 °/s.

Fourier transform infrared (FT-IR) characterization was performed on a Nicolet Avatar 360 instrument (Nicolet, Madison, WI) at 25 °C. The film was firstly grounded with KBr and then vacuum-dried at 40 °C over 48 h to produce disks for the measurements.

Results and discussion

Figure 1 shows the microstructures of the surfaces and the interiors of the regenerated cellulose film, the IIP and the NIIP films. It is observed that the RC film displays homogeneously porous microstructure with a mesh network pattern for both the surface and the inner part, which is similar as the morphology of the regenerated cellulose films reported in the literatures [29, 30]. The surfaces of the IIP and the NIIP films exhibit much denser microstructure, while the inner parts of the films reveal three-dimensional sponge network morphologies. Both of the IIP and the NIIP films have similar porous network microstructures with the same level pore size, which is obviously bigger than that of RC. The porous network

microstructure of the IIP and the NIIP films is consistent with those of the cellulose/alginate blend films [21] or gels [22]. It has been reported that the cellulose/alginate blend films or gels consist of both polymers and the water-soluble alginate were not removed to act as pore former [21, 22], though the exact formation of the mesh porous microstructure has not been clear. We consider that the dehydration and consequently shrinking of both polymers especially the water-soluble alginate during drying would result in the formation of the mesh structure of the films. The dense surfaces of the IIP and the NIIP films are attributed to the cross-linking treatments after coagulation, where the cross-linking reaction took place with priority.

The macroporous mesh structure of the films is beneficial to the transportation of small molecules in their matrix. It has been found that water could easily penetrate into the matrices of the dried IIP and NIIP films, and the equilibrium swelling of both films could be reached within 12 h. The equilibrium swelling ratio of the dried IIP film has been determined to be about 700 %, and that of the NIIP was about 540 %. The higher equilibrium swelling ratio of the IIP film is attributed to the release of cross-linking sites of alginate by the EDTA treatment during preparation. In addition, the IIP film shows satisfactory mechanical properties. The tensile strength (σ_b) and the breaking elongation (ε_b) of the IIP film have been tested to be 45.7 MPa and 5.5 %, respectively.

The IIP film was immersed in Ca^{2+} and Cu^{2+} mixture solution to study its adsorption and competitive ion-recognition. Figure 2 shows the variation of the UV–vis absorbance spectra of the mixture solution with adsorption time. The obvious result is the individually determining of the concentrations of Cu^{2+} and Ca^{2+} in the feed solution at 265 nm and 565 nm, respectively. It is seen that the peak intensity at 265 nm, i.e. the concentration of Cu^{2+} decreases slightly after 45 min. However, the Ca^{2+} concentration peaked at 565 nm in the spectra has been found to decrease greatly with adsorption time. Those results clearly indicate the adsorption of the Ca^{2+} ions prior to the Cu^{2+} ions by the IIP film. Table 1 summarizes the uptake percentages of the feed metal ions, the uptake capacities, the distribution coefficients (K_d) and the selectivity coefficient (K) [31]

Table 1 The parameters of the competitive adsorption of Ca^{2+} and Cu^{2+} by the IIP and the NIIP films

Film	Initial concentration(mg/L)		Uptake (%)		Capacity (mg/g)		K_d (mL/g)		K
	Ca^{2+}	Cu^{2+}	Ca^{2+}	Cu^{2+}	Ca^{2+}	Cu^{2+}	Ca^{2+}	Cu^{2+}	
IIP	20	20	98.4	80.0	2.72	2.54	2.35×10^4	1.53×10^3	15.4
	20	0	99.0	–	2.92	–	5.11×10^4	–	
NIIP	20	20	57.9	65.4	1.08	1.84	4.4×10^2	9.8×10^2	0.45
	20	0	73.2	–	2.12	–	1.10×10^3	–	

Table 2 The absorption of metal ions by the IIP film in Ca^{2+}/Mg^{2+} and Ca^{2+}/Zn^{2+} solutions

Feed solution	Initial concentration (mg/L)	Uptake (%)	Capacity (mg/g)	K_d (mL/g) $\times 10^3$	K
Ca^{2+}/Mg^{2+}	20/20	87.6/56.3	1.84/1.25	0.79/0.14	5.5
Ca^{2+}/Zn^{2+}	20/20	92.1/62.3	1.76/1.17	1.10/0.16	7.1
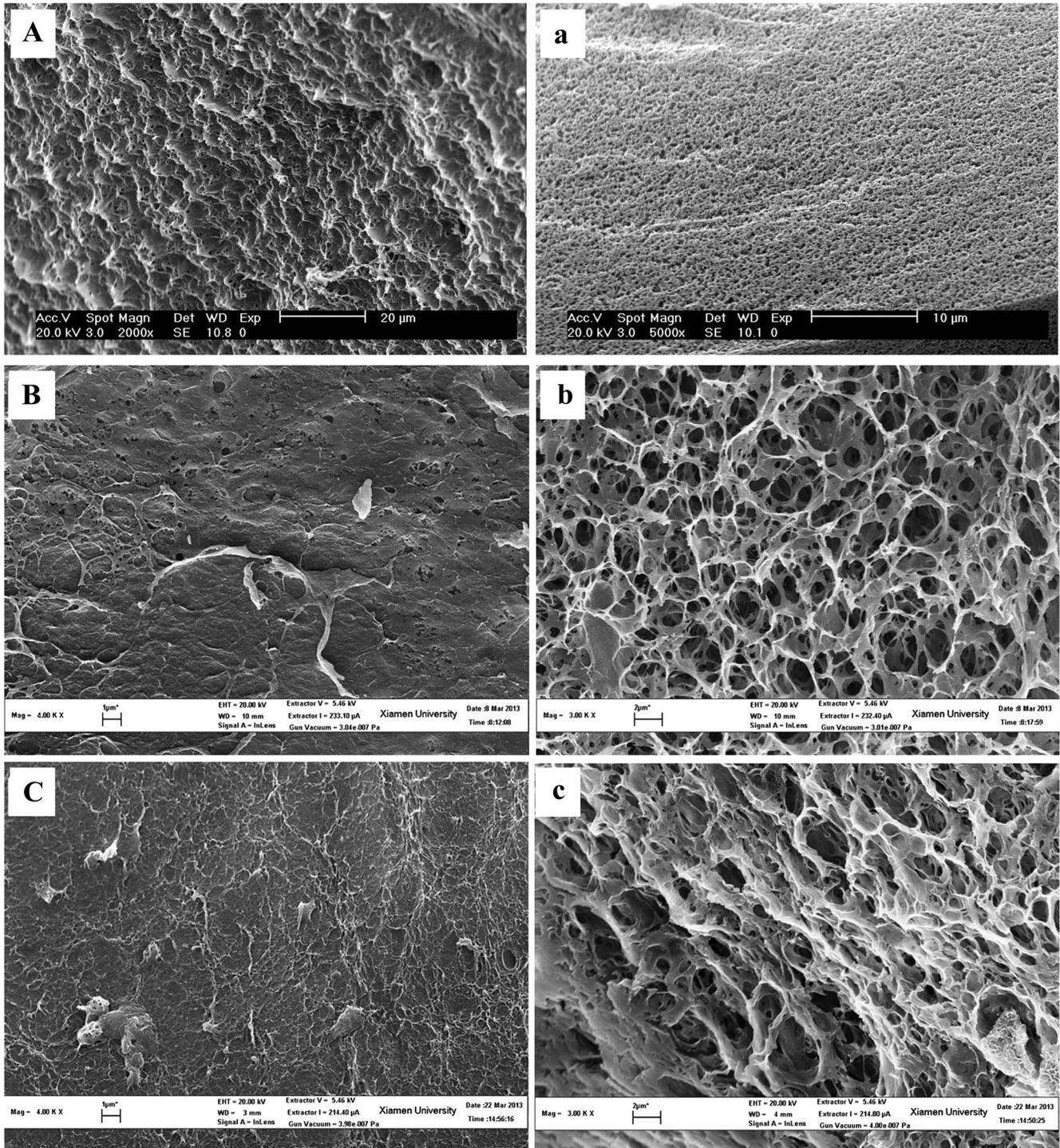
Fig. 1 SEM images of the surfaces (A, B and C) and the corresponding inner parts (a, b and c) for the RC, IIP and NIIP films
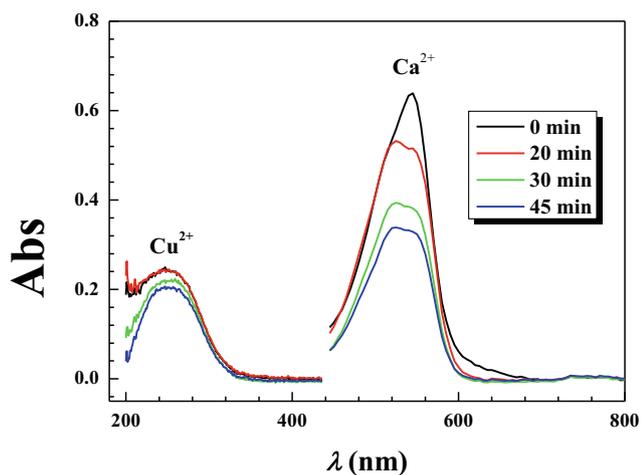
Fig. 2 UV–vis absorbance spectra of the Ca^{2+}/Cu^{2+} mixture solution after adsorption with the IIP film for the indicated time

of the IIP film toward Ca^{2+}. The distribution coefficient (mL/g) is defined as

$$K_d = \frac{(C_i - C_f)V}{C_f W} \qquad (2)$$

Where C_i and C_f are the initial and the final concentrations of the feed ion (mmol/L), V is the volume of the feed solution (mL) and W is the mass of IIP films (g). The selectivity coefficient is the comparison of the distribution coefficients of the competitor ions, i.e.

$$K = \frac{k_d(Ca^{2+})}{k_d(Cu^{2+})} \qquad (3)$$

High K value suggests the prior adsorption of the numerator ion by the adsorbent. Table 1 also lists the corresponding parameters of the NIIP film in order to have a better comparison.

It can be seen that 98.4 % of the Ca^{2+} and 80.0 % of the Cu^{2+} in the mixture feed solution have been adsorbed onto the IIP film, and the adsorption capacities are 2.72 and 2.54 mg/g, respectively. Without the competitive ion of Cu^{2+}, the IIP film has slightly higher uptake and capacity of the Ca^{2+}, suggesting that the presence of the competitive ion of Cu^{2+} with the same charge has limited effect on the adsorption of Ca^{2+}. At the same time, the K_d of Ca^{2+} is found to be much higher than that of Cu^{2+}, and the selectivity coefficient has been calculated to be 15.4, meaning the high Ca^{2+} recognition of the IIP film in the feed solution of mixture ions. The NIIP film also shows some adsorption of the ions based on the functional groups of the polymers, but displays no competitive ion-recognition ($K=0.45$).

Figure 3 shows the uptake kinetic of Ca^{2+} in feed solutions of the Ca^{2+}/Cu^{2+} mixture solution and the Ca^{2+} solution with the same initial Ca^{2+} concentration. The obvious is the overlap

of the data points for the two adsorptions, evidencing little effect of the Cu^{2+} upon the Ca^{2+} recognition of the IIP film once again. The results also indicate that the adsorption of Ca^{2+} took place rapidly, and almost all Ca^{2+} has been extracted within 40 min.

The Ca^{2+} recognition of the IIP film has been further testified by immersing the films into Ca^{2+}/Zn^{2+} and Ca^{2+}/Mg^{2+} mixture solutions, respectively. The competitive ions of Zn^{2+} and Mg^{2+} were chosen because they have the same charge as Ca^{2+} but with different ionic radius. The results of the competitive adsorption of the ions are summarized in Table 2. It is found the IIP film shows a certain extent adsorption capacity to all kinds of ions. However, the selectivity coefficients are 5.5 for the Ca^{2+}/Mg^{2+} and 7.1 for the Ca^{2+}/Zn^{2+}, respectively. Those results clearly indicate the Ca^{2+} recognition of the IIP film. The lower K values of the Ca^{2+}/Mg^{2+} systems than that of the Ca^{2+}/Cu^{2+} is thought to be due to smaller ionic radius of the Mg^{2+} (0.65 Å) which could be adsorbed easier than Cu^{2+} (0.72 Å). Compared with Ca^{2+}/Cu^{2+} system, the Ca^{2+}/Zn^{2+} system shows a lower K with similar size between Zn^{2+} (0.74 Å) and Cu^{2+} (0.72 Å). This may be due to the presence of Zn^{2+} tends to lower the total metal uptake in two-metal systems, while Cu^{2+} has little influence on Ca^{2+}/Cu^{2+} system [32].

The FT-IR spectrum of the IIP film and that of the film after adsorption of Ca^{2+} are shown in Fig. 4. The spectrum of the IIP film shows the characteristic peak of the antisymmetric and symmetric stretching vibration of carboxyl group for SA at 1642 cm^{-1} and 1430 cm^{-1}. The broad bands around 3430 cm^{-1} is attributed to the formation of new hydrogen bonding between the two components, which is consistent with those of the cellulose/SA blends reported in literatures [21]. After adsorption of Ca^{2+}, the spectrum of the film shows a relatively strong and new band peaked at 1560 cm^{-1}, which
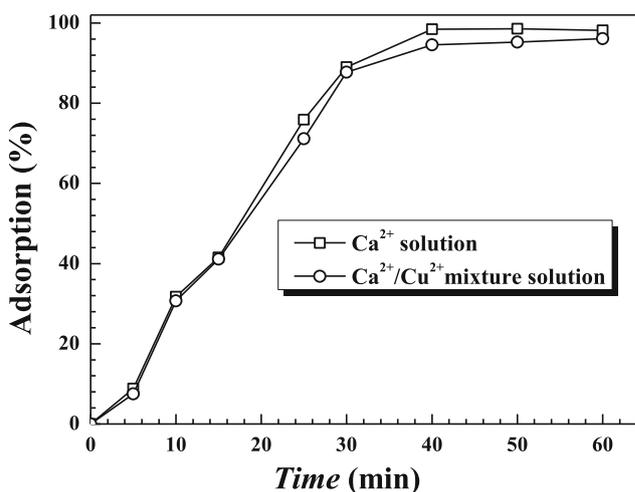
Fig. 3 The uptake kinetic of Ca^{2+} in feed solutions of the Ca^{2+}/Cu^{2+} mixture solution and the pure Ca^{2+} solution. The data points are connected respectively to guide the eyes
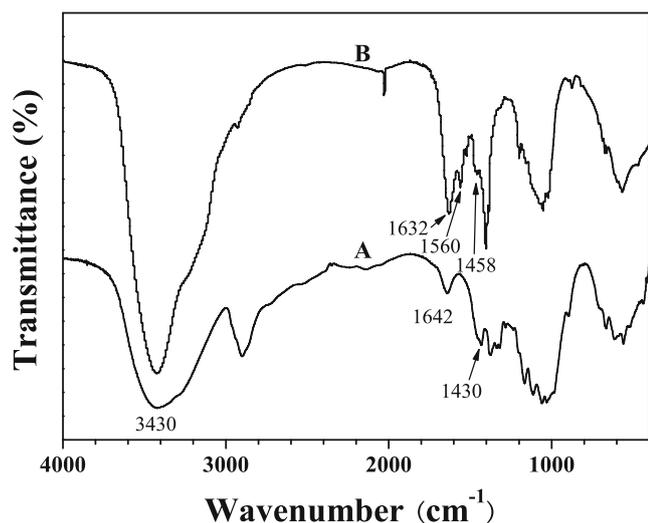
Fig. 4 FT-IR spectra of the IIP (A) and the IIP films after ion-imprinted with Ca^{2+} (B)

is attributed to the presence of Ca^{2+} in the film. Moreover, the characteristic bands of carboxyl group for SA has been found to shift to 1632 cm^{-1} and 1458 cm^{-1}, meaning the chelate formation between the carboxyl groups of SA and the Ca^{2+} [33]. This further confirms why the uptake kinetics failed to fit Langmuir isotherm adsorption in Fig. 3. It is because of the chelating, the IIP film has the property to recognize Ca^{2+}.

The crystalline structure of the IIP film has been studied in order to know more details of its Ca^{2+} recognition. Figure 5 shows the XRD patterns of the regenerated cellulose, the SA and the IIP film. The pattern of RC exhibits diffraction peaks at $2\theta=22°$ and 24°, corresponding to cellulose II crystal structure [34]. The SA shows a peak at around 14°, while the peak at $2\theta=23°$ [35] is not obvious. It is found that the IIP film exhibits no obvious crystalline peak except the broad diffraction band at about 22°, and the intensity of the band is much lower than those of RC peaks. This result suggests the
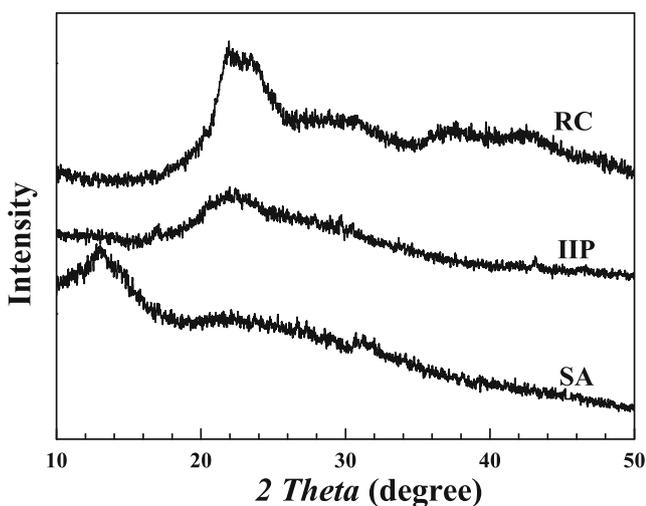
presence of SA would interfere with the crystallization of cellulose in the film, leading to amorphous morphology of the IIP film. Combining with the SEM results, the preparation and the recognition of the IIP film is suggested in Fig. 6. Firstly, the solution mixed two polymers was coagulated in aqueous $CaCl_2$ solution. The compatible cellulose and SA would form the homogeneously mesh network microstructure of the film. Simultaneously, the carboxyl groups of the evenly dispersed SA would chelate with Ca^{2+} in the coagulation bath. Then the film was strengthened by cross-linker of ECH. After that, the Ca^{2+} was removed by EDTA treatment to retain the chelating sites in the film, which could be used for the recognition of Ca^{2+}. Therefore, this work provides an easy method to prepare Ca^{2+} imprinted film, which would have potential applications in fields such as hard water softening, and Ca^{2+} enrichment and recognition.

Conclusions

An ion-imprinted film has been successfully prepared from cellulose and alginate through solution blending. The IIP film exhibits satisfactory mechanical properties for its application. The SEM characterization indicates porous mesh network microstructure of the film, which is helpful to the swelling of the film and to the transportation of small solute in the matrix. Most importantly, the IIP film displays highly selective Ca^{2+} recognition, in the presence and/or in the absence of other metal ions. Detail analysis suggests that compatible cellulose and SA weaved the porous matrix of the film, which was then fixed with chemical cross-linker of ECH. The following extraction of the Ca^{2+} from the film leaves the chelating sites for its post-recognition. Therefore, our work provides an easy way to prepare a Ca^{2+} imprinted film, which would have potential applications in fields such as hard water softening, and Ca^{2+} enrichment or recognition.

Fig. 5 XRD patterns of the films
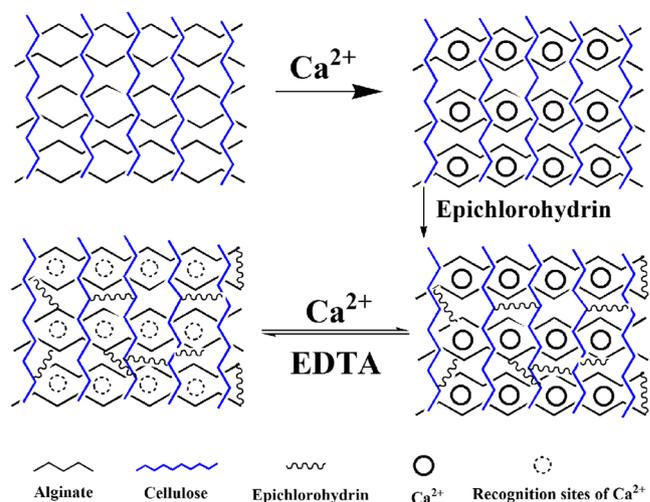
Fig. 6 Schematic preparation of the Ca^{2+} imprinted film

References

1. Pan J, Hu W, Dai X, Guan W, Zou X, Wang X, Huo P, Yan Y (2011) Molecularly imprinted polymers based on magnetic fly-ash-cenosphere composites for bisphenol A recognition. J Mater Chem 21:15741–15751

2. Wulff G (2013) Forty years of molecular imprinting in synthetic polymers: origin, features and perspectives. Microchim Acta 180: 1359–1370

3. Xu S, Chen L, Li J, Wei Q, Ma J (2011) Preparation of hollow porous molecularly imprinted polymers and their applications to solid-phase extraction of triazines in soil samples. J Mater Chem 21:12047–12053

4. Amut E, Fu Q, Fang Q, Liu R, Xiao AP, Zeng AG, Chang C (2010) In situ polymerization preparation of chiral molecular imprinting polymers monolithic column for amlodipine and its recognition properties study. J Polym Res 17:401–409

5. Wu YZ, Zhuang LZ, Ma BB, Chen SX, Xu XZ, Zeng YQ (2014) Preparation of a surface molecularly imprinted fiber for bisphenol a recognition. J Polym Res 21:468. doi:10.1007/s10965-014-0468-6

6. Ozkara S, Andac M, Karakoc V, Say R, Denizli A (2011) Ion-imprinted PHEMA based monolith for the removal of Fe^{3+} ions from aqueous solutions. J Appl Polym Sci 120:1829–1836

7. Yalinca Z, Yilmaz E, Bullici FT (2012) Evaluation of chitosan tripolyphosphate gel beads as bioadsorbents for iron in aqueous solution. J Appl Polym Sci 125:1493–1505

8. Monier M, Abdel-Latif DA (2013) Synthesis and characterization of ion-imprinted resin based on carboxymethyl cellulose for selective removal of $UO2^{2+}$. Carbohydr Polym 97:743–752

9. Zheng X, Fan R, Zhao J (2012) An ion-imprinted microporous polypropylene membrane for the selective removal of Cu(II) from an aqueous solution. Sep Sci Technol 47:1571–1582

10. Vatanpour V, Madaeni SS, Zinadini S, Rajabib HR (2011) Development of ion imprinted technique for designing nickel ion selective membrane. J Membr Sci 373:36–42

11. Saatcilar O, Satiroglu N, Say R, Bektas S, Denizli A (2006) Binding behavior of Fe^{3+} ions on ion-imprinted polymeric beads for analytical applications. J Appl Polym Sci 101:3520–3528

12. Zhao J, Han B, Zhang Y, Wang D (2007) Synthesis of Zn(II) ion-imprinted solidphase extraction material and its analytical application. Anal Chim Acta 603:87–92

13. Behbahani M, Barati M, Bojdi MK, Pourali AR, Bagheri A, Tapeh NAG (2013) A nanosized cadmium(II)-imprinted polymer for use in selective trace determination of cadmium in complex matrices. Microchim Acta 180:1117–1125

14. Kalal HS, Taghiof M, Hoveidi H, Pakizvand N, Vahidi H, Panahi HA, Tavangari S (2013) The Pre-concentration and determination of Iridium and Palladium in environmental water by imprinted polymer-based method. Int J Environ Sci Technol 10:1091–1102

15. Jiang M, Shi Y, Zhang RL, Shi CH, Peng Y, Huang Z, Lu B (2009) Selective molecularly imprinted stationary phases for bisphenol A analysis prepared by modified precipitation polymerization. J Sep Sci 32:3265–3273

16. Lee KY, Mooneya DJ (2012) Alginate: properties and biomedical applications. Prog Polym Sci 37:106–126

17. Sikorski P, Mo F, Skjåk-Bræk G, Stokke BT (2007) Evidence for egg-box -compatible interactions in calcium-alginate gels from fiber X-ray diffraction. Biomacromolecules 8:2098–2103

18. Braccini I, Pérez S (2001) Molecular basis of Ca^{2+}-induced gelation in alginates and pectins: the egg-box model revisited. Biomacromolecules 2:1089–1096

19. Zhu H, Srivastava R, McShane MJ (2005) Spontaneous loading of positively charged macromolecules into alginate-templated polyelectrolyte multilayer microcapsules. Biomacromolecules 6:2221–2228

20. Yang G, Zhang LN, Peng T, Zhong W (2000) Effects of Ca^{2+} bridge cross-linking on structure and pervaporation of cellulose/alginate blend membranes. J Membr Sci 175:53–60

21. Zhou JP, Zhang LN (2001) Structure and properties of blend membranes prepared from cellulose and alginate in NaOH/urea aqueous solution. J Polym Sci Part B: Polym Phys 39:451–458

22. Chang C, Duan B, Zhang LN (2009) Fabrication and characterization of novel macroporous cellulose-alginate hydrogels. Polymer 50: 5467–5473

23. Cai J, Zhang LN (2006) Unique gelation behavior of cellulose in NaOH/urea aqueous solution. Biomacromolecules 7:183–189

24. Cai J, Zhang LN, Zhou JP, Qi HS, Chen H, Kondo T, Chen X, Chu B (2007) Multifilament fibers based on dissolution of cellulose in NaOH/urea aqueous solution: structure and properties. Adv Mater 19:821–825

25. Yu ZJ, Jiang YQ, Zou WW, Duan JJ, Xiong XP (2009) Preparation and characterization of cellulose and konjac glucomannan blend film from ionic liquid. J Polym Sci Part B: Polym Phys 47:1686–1694

26. Zhou Y, Wang F, Kim Y, Kim SJ, Yoon J (2009) Cu^{2+}-selective ratiometric and "off-on" sensor based on the rhodamine derivative bearing pyrene group. Org Lett 11:4442–4445

27. Cheng F, Zhang Y, Chang H, Dong C (2006) UV spectrophotometric determination of magnesium and calcium in brine from saltlake. Inorg Chem Ind 4:54–56

28. Ramkumar J, Maiti B, Mathur PK (1998) Use of masking agents in promoting selective transport of Zn^{2+} through nafion membrane. Sep Sci Technol 33:2423–2429

29. Mao Y, Zhou JP, Cai J, Zhang LN (2006) Effects of coagulants on porous structure of membranes prepared from cellulose in NaOH/urea aqueous solution. J Membr Sci 279:246–255

30. Xiong XP, Duan JJ, Zou WW, He XM, Zheng W (2010) A pH-sensitive regenerated cellulose membrane. J Membr Sci 363:96–102

31. Wang Z, Wang M, Wu G, Shen Y, He C (2010) Ion imprinted sol–gel nanotubes membrane for selective separation of copper ion from aqueous solution. Microchim Acta 169:195–200

32. de Carvalho RP, Chong KH, Volesky B (1995) Evaluation of the Cd, Cu and Zn biosorption in two-metal systems using an algal biosorbent. Biotechnol Prog 11:39–44

33. Huang RYM, Pal R, Moon GY (1999) Characteristics of sodium alginate membranes for the pervaporation dehydration of ethanol-water and isopropanol-water mixtures. J Membr Sci 160:101–113

34. Mao Z, Cao Y, Jie X, Kang G, Zhou M, Yuan Q (2010) Dehydration of isopropanol-water mixtures using a novel cellulose membrane prepared from cellulose/N-methylmorpholine-N-oxide/H2O solution. Sep Purif Technol 72:28–33

35. Fan LH, Du YM, Huang RH, Wang Q, Wang X, Zhang LN (2005) Preparation and characterization of alginate/gelatin blend fibers. J Appl Polym Sci 96:1625–1629